Catal Lett (2018) 148:277–288
DOI 10.1007/s10562-017-2220-4

Green Synthesis of Pd Nanoparticles Supported on Magnetic Graphene Oxide by *Origanum vulgare* Leaf Plant Extract: Catalytic Activity in the Reduction of Organic Dyes and Suzuki–Miyaura Cross-Coupling Reaction

Neda Seyedi[1] · Kazem Saidi[1] · Hassan Sheibani[1]

Received: 13 July 2017 / Accepted: 1 October 2017 / Published online: 23 October 2017

Abstract A novel and green approach based on the biosynthesis of palladium nanoparticles on modified graphene oxide by *Origanum vulgare* leaf plant extract have been developed by our group. The prepared magnetically nanocatalyst was characterized by transmission electron microscopy, scanning electron microscopy, X-ray diffraction, vibrating sample magnetometer (VSM) and Fourier transform infrared spectroscopy. The heterogeneous catalytic system was investigated for the reduction of 4-nitrophenol, methylene blue and methyl orange in the presence of $NaBH_4$ as a reducing reagent and also for Suzuki–Miyaura cross-coupling reactions between phenylboronic acid and a range of aryl halides (X = I, Br, Cl). Moreover, synthesized catalyst could be readily recycled and reused several times without significant loss of activity.

Graphical Abstract

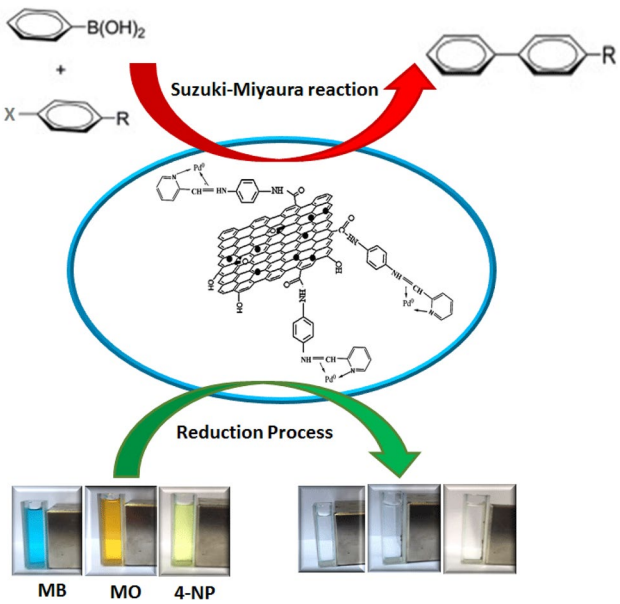

Keywords Leaf extract · GO/Fe_3O_4/Pd nanocomposite · Reusability · *Origanum vulgare* · Cross-coupling reactions

1 Introduction

Metal-catalyzed cross-coupling reactions have become one of the most powerful reactions in the organic synthesis [1–3]. In particular, Pd-catalyzed cross-coupling has been efficiently used in numerous procedures for the constructions of C–C and C–N bonds [4–9]. Suzuki–Miyaura (SM) cross-coupling introduces one of the most developed methods which have been reported for the synthesis of biaryls [10]. These compounds are important for the preparations

✉ Hassan Sheibani
Hsheibani@uk.ac.ir

[1] Department of Chemistry, Shahid Bahonar University of Kerman, Kerman 76169, Iran

of biologically active molecules [11] and also were widely used and applied to numerous areas such as pharmaceuticals, agrochemical [12] and herbicides [13] industry.

Homogeneous metal catalysts are frequently used in the laboratory to perform experimental coupling reactions, [14] but they do not have industrial applications due to the difficulty in separating and recycling the catalyst. In addition, recyclability of homogeneous metal catalysts is considered as a major objective in relation to green chemistry [15]. In order to solve these problems, new strategies should be developed [16–19] that involve the immobilization of homogeneous metal catalysts onto solid supports. Recently the solid materials, such as activated carbon [20–22], zeolites [23–25] and nanoparticles [26, 27] have been used as solid supports for the homogeneous catalysts. Nowadays, the chemically modified graphene or graphene oxide have been applied in the preparation of organic compounds as a solid support. A few papers are found which used graphite (G) or graphene oxide (GO) as a solid support for palladium ions and/or palladium nanoparticles catalyst in the C–C cross-coupling reactions [28–30]. Graphene oxide (GO) can be easily exfoliated in aqueous media to yield stable dispersions of mostly single-layer sheets of GOs, which is the most versatile and effective method. It contains reactive oxygen functional groups such as epoxy and hydroxyl groups on basal planes and carboxylic acid groups at its edges to obtain novel multi-functional nanomaterials [31, 32]. Since GO has strong hydrophilicity property therefore it can be easily dispersed in water and forms strong interlayer hydrogen bonds between mentioned oxygen functional groups [33, 34]. This problem can be solved by the functionalization of GO nanosheets with organic moieties; subsequently further stabilizing can be achieved by the growth of ligand chains. On the other hand, the catalytic activity of Pd^{2+}-modified graphene oxide decreased gradually when the catalyst was used repeatedly because the interaction between palladium and the support material will be weak [27, 28].

Therefore, to improve the stability and catalytic activity of this catalyst, Immobilized Pd^{2+} on the surface is reduced to Pd nanoparticles, which several methods have been used for the syntheses of palladium nanoparticles, these methods suffer some drawbacks such as use of high temperature and pressure along with producing of hazardous by-product [35]. The plant extracts for the synthesis of Pd nanoparticles have been proposed as a valuable alternative to chemical methods to avoid from cited disadvantages. There are a few available reports for the synthesis of palladium nanoparticles (Pd-NPs) that effectively used from planets such as: *Soybean* (*Glycine max*) leaf extract [36], *Cinnamomum zeylanicumbark* [37], *C. camphora* leaf [38], *Curcuma longa tuber* [39], *Pistacia atlantica, Kurdica* Gum [40], *Pectin* [41] and *Stachys lavandulifol* [42].

In this research group, the synthesis of Pd nanoparticles was used *Origanum vulgare* leaf extract which is belongs to Lamiaceae family (Fig. 1). It is an indigenous in Cyprus and southern Turkey, and was known to the Greeks and Romans as a symbol of happiness grows well in Central Asia, Iran, India, Turkey, Afghanistan, Pakistan and in many parts of the world. In this plant, over 60 different compounds have been identified. On the other hand, insertion of magnetic Fe_3O_4 nanoparticles in to Pd NPs grafted GO, which cause easier separation and recovery of the Pd magnetic nanoparticles in comparison to nanocatalyst without magnetic property.

In this research, Pd NPs were complexed with grafted imine to GO as a schiff base ligand that was modified on graphene oxide. The schiff base complexes are suitable choices for the preparation of nanoparticle, which have unique chemical, and optical properties. The catalytic activity of the prepared catalyst was investigated by employing Suzuki–Miyaura coupling reaction, reduction of 4-nitrophenol and dyes such as MO, MB as model reactions. The results show that the reactivity of new prepared heterogeneous catalyst is similar to a homogeneous catalyst. This catalyst was easily separated from reaction mixture without significant decrease in catalytic activity.

2 Experimental

2.1 Materials and Chemical Instruments

Graphite, potassium permanganate ($KMnO_4$), sodium nitrate ($NaNO_3$), hydrochloric acid (HCl), sulfuric acid (H_2SO_4), peroxide hydrogen (H_2O_2), thionyl chloride

Fig. 1 Images of *Origanum vulgare*

($SOCl_2$), 1,4-phenylene diamine (1,4-PDA), 2-pyridine carboxaldehyde, palladium chloride ($PdCl_2$), ferric chloride hexahydrate ($FeCl_3{\cdot}6H_2O$), ferrous chloride tetrahydrate ($FeCl_2{\cdot}4H_2O$), phenylboronic acid, various aryl halide, 4-nitro phenol (4-NP), methylene blue (MB), methyl orange (MO), ammonia (NH_3), potassium carbonate (K_2CO_3), triethylamine (TEA) and solvents were purchased from Merck and Aldrich chemical companies and used without further purification, *O. vulgare* plant was obtained from Dalfard area, (City of Jiroft, Province of Kerman, Iran).

Infrared (IR) spectra were recorded with KBr pellet on a Bruker tensor 27 Fourier transform infrared (FT-IR) spectrometer with RT-DLATGS detector, in the range of 400–4000 cm^{-1} with a spectral resolution of 4 cm^{-1} in transmittance mode. The powder X-ray diffraction (XRD) patterns were examined on a model X'PertPro diffractometer (Panalytical, Almelo, the Netherlands) using Cu Kα radiation (wavelength = 1.54 Å). The data were collected over a range of 10–80° 2θ with a step size of 0.01°, nominal time per step of 2 s and slit width 5 nm. Ultraviolet–visible (UV–Vis) spectroscopy was performed in the range of 200–900 nm on a Cary 50 single detector double beam in time spectrophotometer (Varian, Australia). The morphologies and sizes of the prepared samples were characterized by A LEO 912AB transmission electron microscopy (TEM), (Carl Zeiss Inc., Jena, Germany) and was used with an accelerating voltage of 100 kV. Scanning electron microscopy (SEM) and energy-dispersive X-ray spectroscopy (EDS) were carried out using SIGMA VP from Carl Zeiss Inc., Jena, Germany.

2.2 Synthesis

2.2.1 Preparation of Leaf Extract

Freshly collected *O. vulgare* leaves were collected in July 2016 in Dalfard region of Kerman province in Iran. 5.0 g of the dry powdered samples with 100 mL ethanol as a solvent well mixed and then boiled for 30 min, and thereafter filtrated, ethanol solvent was evaporated by rotary evaporator and yielded dark greenish powder. Then the extract was kept in sterile bottles and put in refrigerator at 3–5 °C until further use.

2.2.2 Preparation of the Fe_3O_4 Magnetic Nanoparticles (MNPs)

The magnetic nanoparticles were synthesized at the required stoichiometric ratios of Fe^{3+}/Fe^{2+} (3:2) by chemical co-precipitation method [43].

2.2.3 Preparation of Graphene Oxide (GO)

Graphene oxide was synthesized from commercially obtained graphite by Hummers method for preparation of modified GO [44, 45].

2.2.4 Preparation of Amine Functionalized Graphene Oxide (GO–NH_2)

In a typical procedure, initially GO (500 mg) and $SOCl_2$ (50 mL) were added to a round bottom flask. The mixture was refluxed at 70 °C for 48 h under nitrogen atmosphere, in order to generate GO–Cl. The excess amount of $SOCl_2$ was removed by distillation under reduced pressure and the remaining solid washed with dry dimethylformamide (DMF) several times. Then, the obtained solid was dispersed in anhydrous DMF and further reacted with 5 mmol of 1,4-PDA and 5 mmol of triethylamine (TEA) under nitrogen atmosphere for 12 h. The resulting mixture was subsequently separated by centrifugation and washed with anhydrous dimethylformamider, and dried at vacuum oven at 40 °C to yield amine-terminated GO which titled as GO–NH_2.

2.2.5 Preparation of Imine Grafted Modified Graphene Oxide (GO–NH=C)

The obtained (GO–NH_2) in previous section were treated with 2-pyridine carboxaldehyde (5 mmol) in methanol (20 mL), in order to introduce imine groups to the modified graphene oxide surface, the reaction mixture were refluxed for 8 h, the (GO–NH=C) were separated successively with centrifuge and dried under vacuum.

2.2.6 Preparation of Pd Nanoparticles Grafted Modified GO (GO–NH=C)–Pd NPs

For the preparation of (GO–NH=C)–Pd NPs, 500 mg powder of (GO–NH=C) was dispersed in acetonitrile and heated to 45 °C with mechanical stirring. The $PdCl_2$ solution (10 mg $PdCl_2$ was pre-dissolved in 50 mL acetonitrile) was added to the above mixture and stirred at 45 °C for 12 h, then leaf extract of *O. vulgare* (2.5% w/v) (8 mL) was added to the stirring reaction mixture and stirring was continued for an additional 6 h in order to prepare Pd nanoparticles. The residual precipitates were centrifuged and washed three times with acetonitrile and dried under vacuum.

2.2.7 Preparation of Magnetic Nanocomposite (GO/Fe_3O_4/Pd Nanocomposite)

Prepared Fe_3O_4 NPs (200 mg) was dispersed in 20 mL of acetonitrile by ultrasonication. The dispersed (GO–NH=C)–Pd NPs (100 mg) in acetonitrile (20 mL) was

added to the prepared suspension of Fe_3O_4 NPs and stirred at 50 °C for 7 h. The reaction mixture was cooled down to an ambient temperature. The prepared catalyst was collected using an external magnet and washed with distilled water.

2.3 General Producer for Reduction of Dyes by (GO/Fe_3O_4/Pd Nanocomposite)

2.3.1 Catalytic Reduction of 4-Nitrophenol (4-NP)

The reduction of 4-NP in the presence of an excess amount of $NaBH_4$ was studied in a standard quartz cell and monitored by a UV–Vis spectroscopy in the range of 250–600 nm. The analysis procedure is described as following: 2 mL of distilled water, 1 mL of freshly prepared aqueous $NaBH_4$ solution (0.2 mol/L) and 0.1 mL of 4-NP (5 mmol/L) were added into a quartz cell and the solution was turned to yellow color. Afterward, 1 mg of GO/Fe_3O_4/Pd nanocomposite (3.9×10^{-5} mg Pd) quickly was transferred into the cell and absorbance evolution was recorded after different intervals time, until the absorbance became constant. In order to study the reusability of catalyst, it was separated from the solution by an external magnet after completed reduction process, The recycled used catalyst was then washed several times with distilled water and used for ten times.

2.3.2 Catalytic Reduction of MB and MO

In a typical experiment to 4 mL stirring aqueous solution of MB (1.6×10^{-6} M) or MO (2.4×10^{-5} M), 1 mg catalyst GO/Fe_3O_4/Pd nanocomposite (3.9×10^{-5} mg Pd) was added, following by addition of 2 mL prepared aqueous solution $NaBH_4$ (0.2 M) at room temperature. The progress of the reaction was monitored by the change of the absorption intensity in UV–Vis spectrophotometer in the range of 400–750 nm. After completion of the reaction, the catalyst was separated from the reaction mixture by an external magnet and washed successively with distilled water and ethanol then dried for the next run. In order to the reusability of the recycled catalyst, it was used for 10 times and no extensive change was observed.

2.3.3 General Procedure for Suzuki–Miyaura Cross Coupling of Aryl Halides with Phenylboronic Acid in the Presence of (GO/Fe_3O_4/Pd Nanocomposite)

In a typical reaction, the catalyst of GO/Fe_3O_4/Pd nanocomposite (0.5 mol%) was placed in a 10 mL schlenk tube and a solution of Water/EtOH (4 mL) was added to the reaction mixture which involve aryl halides (1 mmol), phenylboronic acid (1.1 mmol) and K_2CO_3 (2 mmol). The reaction mixture was stirred for the desired time at 80 °C and monitored using TLC. The reaction mixture was cooled to room temperature after completion and the catalyst was separated by external magnet then extracted with ethyl acetate (3×10 mL). The obtained organic solution was dried over anhydrous sodium sulfate and evaporated in a rotary evaporator under reduced pressure. The crude product was purified by column chromatography (silica gel particle size 0.2–0.5 mm—35–70 mesh ASTM, *n*-hexane) and the turnover number (TON (= mol of product/mol of catalyst)) and turnover frequency [TOF (= TON/time (h))] were calculated on the basis of the amount of biaryl product formed.

3 Result and Discussions

3.1 Synthesis

The main goal of this study was to design a new magnetic Pd NPs grafted to modified GO. The GO exhibits enormous active edges and oxygen functional groups on its basal plane, moreover, these functional groups provide reactive sites for producing Pd NPs and also make it easily dispersible in aqueous solution. The fabrication of GO/Fe_3O_4/Pd nanocomposite essentially includes six steps, as illustrated in Fig. 2. Initially, GO was produced from natural flake graphite (400 nm) by a modified Hummers method [46], in which contains mixture of single-layer and a few-layer GO in solution [47]. The carboxylic acid groups of GO was acylated in the presence of excess $SOCl_2$ in order to react with 1,4-phenylenediamine. In this work, to graft Pd on modified GO, we need to add functional groups which can be coordinated with Pd. For this purpose 1,4-diamine derivatives were selected, which in first, to form amide group, one of the amino groups of 1,4-diamine derivatives reacted with acylchloride on GO and other amine group reacting with 2-pyridine carboxaldehyde to yield imine group. The Pd^{2+} ion was coordinated with imine groups and reduced by leaf extract of *O. vulgare* to form Pd NPs. Since the separation and recovery of (GO–NH=C)–Pd NPs were difficult due to high suspensibility GO, this catalyst was magnetized by Fe_3O_4 NPs.

3.2 Characterization

The FT-IR spectrum of GO in Fig. 3a shows a strong absorption band at 1716 cm^{-1} due to C=O stretching of the –COOH group and the stretching vibrations of C–O group of the epoxy, and carboxylic acid at 1220 and 1042 cm^{-1} were appeared respectively. It also exhibits a band around 1617 cm^{-1} attributable to the vibrations of C=C in the GO [48]. After the functionalization process and formation of amine groups on modified GO (GO–NH_2) in Fig. 3b shows the presence of the new bands at 1656 and 1536 cm^{-1} corresponding to carbonyl group of amide and –C–N stretching

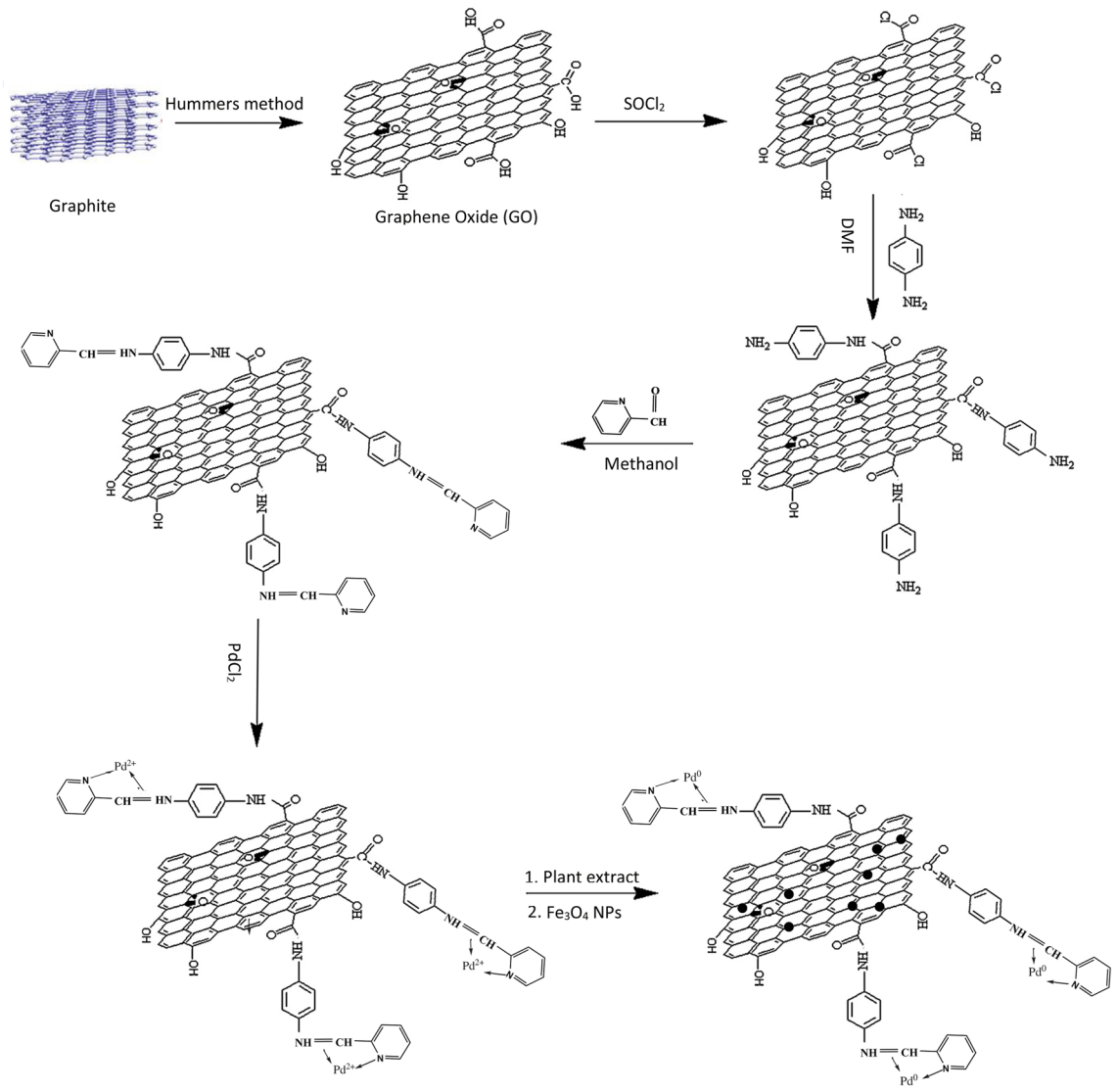

Fig. 2 Formation process of (GO/Fe_3O_4/Pd nanocomposite)

[49, 50]. After doing imination reaction of GO–NH_2 with 2-pyridine carboxaldehyde, two new peaks around 1642 and 1549 cm^{-1} appeared, which were attributed to the vibrations of C=N groups (formed imine and pyridine ring) shown in Fig. 3c. These results indicated that the 1,4-phenylenediamine was bonded to the surface of GO through amidation reaction. The IR scanning patterns of (GO–N=C)–Pd NPs and (GO–N=C) samples were almost similar indicating that the structure of imine bonded to modified GO preserved the process of coordination and reduction shown in Fig. 3d. After magnetization of catalyst a band at 569 cm^{-1} appeared which is related to stretching mode of Fe–O in Fe_3O_4 nanoparticles in (GO/Fe_3O_4/Pd nanocomposite) shown in Fig. 3e.

The formation of (GO/Fe_3O_4/Pd nanocomposite) and the crystallinity of the nanocomposite were further confirmed by XRD analysis. For this purpose, XRD patterns of (GO/Fe_3O_4/Pd nanocomposite) were measured (Fig. 4) and showed several peaks at $2\theta = 10$, 30.2, 35.5, 40.02, 43.1, 44.5, 46.49, 53.4, 57.1, 62.8, 68.05 and 81.74 that the peak centered at $2\theta = 10.1$ corresponding to the (001) crystal planes are almost the same as that of pure GO [51]. The peaks at $2\theta = 30.2$, 35.5, 43.1, 44.5, 53.4, 57.1 and 62.8, are related to (111), (2 2 0), (311), (4 0 0), (4 2 2), (511) and (4 4 0) crystallographic faces were observed in the case of Fe_3O_4 NPs [52]. So the obvious diffraction peaks at $2\theta = 40.02$, 46.49, 68.05, 80.74 and 85.5 can be attributed to the reflections of the 111, 200, 220, 311 and 222 crystalline planes of cubic Pd, respectively [53].

The typical morphologies of the resulting GO/Fe_3O_4/Pd nanocomposite were observed by FE-SEM and TEM, as exhibited in Fig. 5. The FE-SEM image of the GO/Fe_3O_4/Pd nanocomposite shown in Fig. 5b, exhibits the layer-by-layer

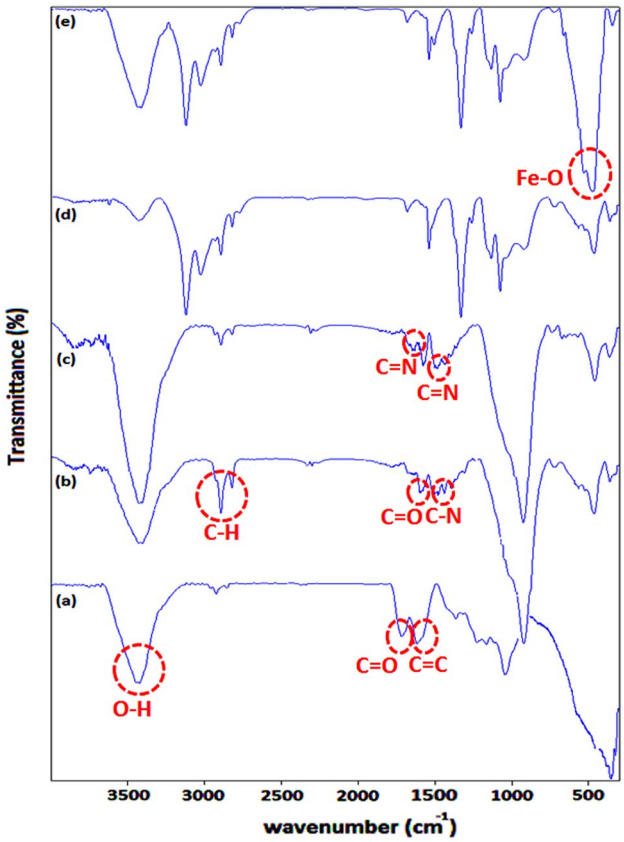

Fig. 3 FT-IR spectra of (*a*) GO, (*b*) GO–NH_2, (*c*) (GO–N=C), (*d*) (GO–N=C)–Pd, (*e*) (GO/Fe_3O_4/Pd nanocomposite)

structure of GO in stacking with a size micrometers and the nanosheet morphologies that is similar to the SEM image of the pure GO shown in Fig. 5a indicates the presence of the Pd and Fe_3O_4 NPs has verified by appearing as some bright spots in the surface of modified GO, which indicating that this composite has been successfully synthesized. A typically TEM shows that iron oxide and Pd nanoparticles were successfully coated on the surface of the GO to form a GO/Fe_3O_4/Pd nanocomposite and the size of nanoparticles ranged from 10 to 40 nm (Fig. 5c, d). EDS analysis (Fig. 5e) clearly shows the presence of Pd and Fe in the GO/Fe_3O_4/Pd nanocomposite catalyst as well as the presence of carbon with an insignificant amount of oxygen probably due to the oxygen functional groups have been shown.

The magnetic properties of the catalyst were characterized using a SQUID magnetometer measured at room temperature (298 K) as shown in Fig. 6. The amount of magnetization saturation (Ms) value in this catalyst is 27.8 emu/g in compared with bare Fe_3O_4 NPs (69.9 emu/g). It should be noted that the catalyst shows strong magnetization which is suitable for magnetic separation and recovery.

3.3 Catalytic Studies

3.3.1 Catalytic Activity of GO/Fe_3O_4/Pd Nanocomposite in the Suzuki–Miyaura (SM) Cross Coupling

To investigate catalytic efficacy of the prepared GO/Fe_3O_4/Pd nanocomposite, we have studied the Suzuki–Miyaura cross-coupling reaction of aryl halides with phenylboronic acid in H_2O/EtOH as a green solvent. In this work, the cross-coupling of iodobenzene with phenylboronic acid was chosen as the model reaction (Scheme 1).

To optimize reaction condition, the model reaction was treated under different conditions such as various solvents, bases, temperatures and the amount of nanocatalysts (Table 1). The used solvents such as acetonitrile, DMF, THF, H_2O, EtOH were inefficient for this reaction while the H_2O/EtOH solvent was found as the most effective and greener solvent. And so in the presence of K_2CO_3, the yield of these reactions were high in compared to organic base such as Et_3N. During our optimization studies, the effect of temperature was examined and it was found that this reaction was done at 80 °C with high yield and short

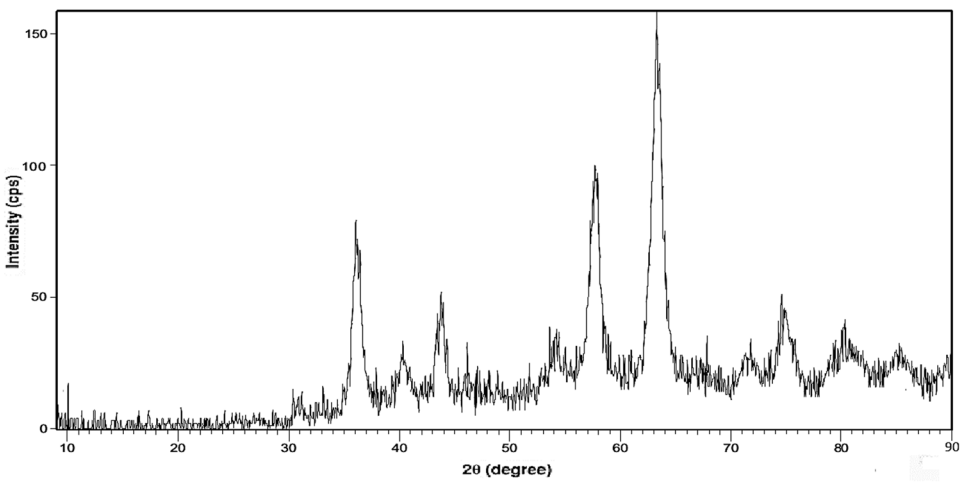

Fig. 4 XRD patterns of (GO/Fe_3O_4/Pd nanocomposite)

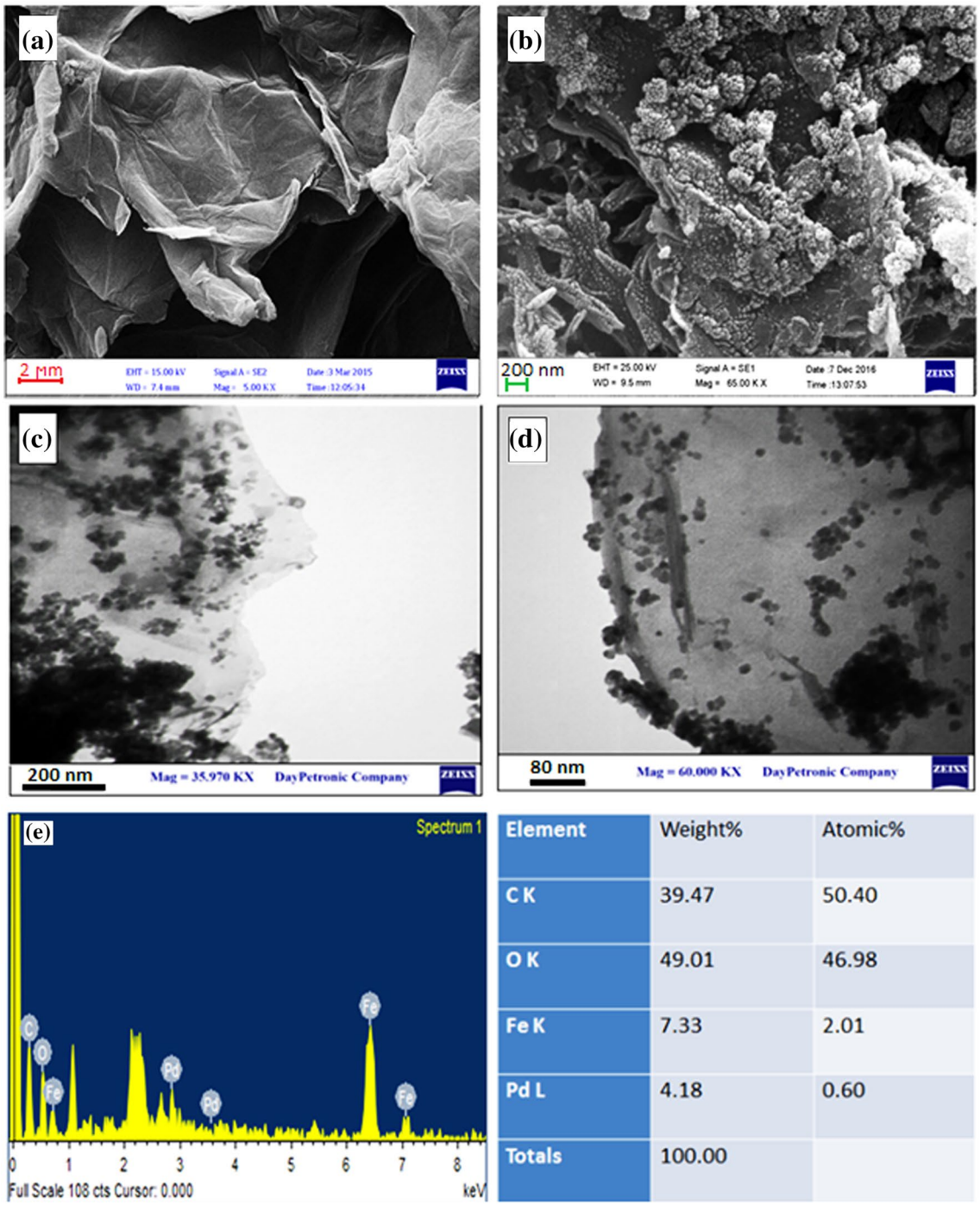

Element	Weight%	Atomic%
C K	39.47	50.40
O K	49.01	46.98
Fe K	7.33	2.01
Pd L	4.18	0.60
Totals	100.00	

Fig. 5 **a** FE-SEM of GO, **b** FE-SEM of GO/Fe_3O_4/Pd nanocomposite, **c, d** TEM of GO/Fe_3O_4/Pd nanocomposite and **e** EDS of GO/Fe_3O_4/Pd nanocomposite

reaction times. Finally the model reaction was carried out in presence of different amounts of catalyst. Variation of amounts catalyst had an effective influence on the product yield. The optimum amount of GO/Fe_3O_4/Pd nanocomposite was found 0.5% mol Pd.

Having optimized the reaction conditions, a variety of aryl halide with different functional groups were chosen as the substrates in this Suzuki–Miyaura cross-coupling reaction, which were performed well for all the examined substrates and the corresponding products were obtained in high

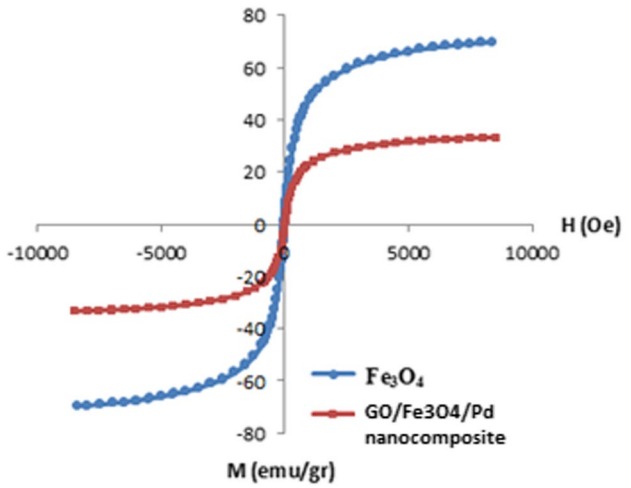

Fig. 6 Magnetization curves of Fe_3O_4 nanospheres and (GO/Fe_3O_4/Pd nanocomposite)

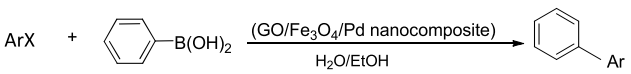

Scheme 1 Suzuki–Miyaura cross-couplings of aryl halides with phenylboronic acid

yields.Several representative coupling reactions involving a variety of aryl halides (I, Br and Cl) and phenylboronic acid in optimized condition (0.5 mol% catalyst, K_2CO_3, H_2O/EtOH, 80 °C) were investigated. The results are summarized in Table 2. It shows aryl iodides bearing electron-withdrawing and electron-donating groups couple efficiently with phenylboronic acid, and generate the corresponding products in good to excellent yields with short reaction times (Table 2, entries 1, 2, 3, 4, 5). The coupling reaction of chlorobenzene with phenylboronic acid requires extended reaction time compared to aryl iodides and bromides, producing the desired product in moderate yield (Table 2, entry 10). The reactions of sterically hindered *ortho*-position halides and bulky 1-bromonaphthalene and 4-bromo-2-fluorobiphenyl with phenylboronic acid also provide good yields of the desired biaryls under the optimized reaction conditions (Table 2, entries 4, 7, 9).

We compared our results with those of the Pd based catalysts reported in the past years for Suzuki–Miyaura coupling reaction, taking the reactions of iodobenzene with phenylboronic acid as an example (Table 3) [54–60]. The reported results have been shown that the catalyst had highest TOF in compare to other catalysts and this reaction was done with high yield in the short reaction time.

3.4 Catalytic Stability and Reusability

To investigate reusability of the GO/Fe_3O_4/Pd nanocomposite in the Suzuki–Miyaura cross-coupling reaction of iodobenzene with phenylboronic acid in the presence of potassium carbonate (K_2CO_3) was chosen as a model reaction (Table 2). Upon completion of the initial reaction, the nanocatalyst was recovered by an external magnet and washed sequentially with ethanol and acetone to remove any impurities, then dried (under vacuum) and reused in the same reaction. The results of these experiments revealed that the activity of GO/Fe_3O_4/Pd nanocomposite retained in the six reaction cycles, without any significant loss in its catalytic activity, According to ICP–AEM, the content of palladium in the sample was confirmed. The weight percentage of palladium in fresh catalyst was 3.9 wt% (0.36 mmol g^{-1}), although it is more than the amount found in the some previous studies [61, 62], but in this study we report GO/Fe_3O_4/Pd nanocomposite as an efficient catalyst with short reaction times and high yields in comparison with previously reports. Also, the weight percentage of palladium for recovered catalyst (after six times) was 3.4 wt% (0.31 mmol g^{-1}). Based on these results, we can conclude that there is little difference in weight percentage of palladium in recovered and fresh catalyst that was used the first time in the reaction, and this

Table 1 Suzuki–Miyaura cross-coupling reaction phenylboronic acid and iodobenzene with (GO/Fe_3O_4/Pd nanocomposite)

Entry	Solvent	Base	Temperature (°C)	Amount of catalyst (mol%)	Time (min)	Yield (%)
1	Acetonitrile	K_2CO_3	80	0.5	10	30
2	THF	K_2CO_3	80	0.5	10	30
3	DMF	K_2CO_3	80	0.5	10	95
4	EtOH	K_2CO_3	80	0.5	10	85
5	H_2O	K_2CO_3	80	0.5	10	85
6	H_2O/EtOH	K_2CO_3	80	0.5	10	95
7	H_2O/EtOH	Et_3N	80	0.5	10	70
8	H_2O/EtOH	K_2CO_3	r.t.	0.5	10	50
9	H_2O/EtOH	K_2CO_3	80	0.36	10	80
10	H_2O/EtOH	K_2CO_3	80	0.72	10	95

Table 2 Synthesis of biphenyl derivatives in the presence of (GO/Fe_3O_4/Pd nanocomposite)

Entry	Compound noun	Arx	X	Time (min)	Yield (%)	TON	TOF
1	3a	C_6H_5	I	10	95	190	1140
2	3b	4-CH_3–C_6H_5	I	15	90	180	720
3	3c	4-OCH_3–C_6H_5	I	15	95	190	760
4	3d	2-OCH_3–C_6H_4	I	20	93	186	558
5	3e	4-NO_2–C_6H_4	I	20	85	170	510
6	3f	4-OCH_3–C_6H_5	Br	30	85	170	340
7	3g	1-Naphty	Br	40	85	170	255
8	3h	4-CH_3CO–C_6H_6	Br	20	85	170	510
9	3i	4-2F-Biphenyl	Br	20	80	160	480
10	3j	C_6H_5	Cl	60	70	140	140

Reaction condition: phenylboronic acid (1.5 mmol), arylhalide (1 mmol), K_2CO_3 (2 mmol), catalyst (0.5 mol% Pd), calculation of TONs and TOFs were cited in the "Experimental" section

Table 3 Comparison of activity for different catalytic systems in C–C cross-coupling Suzuki–Miyaura reaction

Entry	Catalyst	Solvent	Base	Temp (°C)	Time (h)	Yield (%)	TON	TOF	Refs.
1	Pd/MCM 41%	H_2O	K_3PO_4	78	5	93	930	186	56
2	LDH–DS–Pd	DMF/H_2O (5:1)	K_2CO_3	80	0.5	90	18	36	57
3	Pd–IP–IL	H_2O	Na_2CO_3	100	6	90	90	15	58
4	Hollow Pd sphere	ETOH	K_3PO_4	80	3	99	33	11	59
5	Pd NPs	ETOH/H_2O (1:1)	K_2CO_3	80	2	95	325	162.5	60
6	Pd–rGO	ETOH/H_2O (1:1)	NaOH	60	3	92	460	153.3	61
7	Pd–Ni/RGO	EtOH:H_2O (1:1)	K_2CO_3	30	5	98.7	5477	1095	62
8	GO/Fe_3O_4/Pd nanocomposite	ETOH/H_2O (1:1)	K_2CO_3	80	0.15 (10 min)	95	190	1140	This work

small difference does not affect the reaction yield after six times (see Fig. 7). Moreover, this evidence showed that Pd was linked with imine group and nitrogen of pyridine ring with high stable linkages.

3.4.1 Catalytic Activity of GO/Fe_3O_4/Pd Nanocomposite in the Reduction of 4-Nitrophenol, MO, MB

In order to investigate the catalytic activity of GO/Fe_3O_4/Pd nanocomposite, the reduction of 4-nitrophenol, methylene blue and methyl orange were chosen as a model reaction in presence of $NaBH_4$. The reaction can be monitored easily by measuring the change in UV–Vis absorbance at 400 and 300 nm. To compare the catalytic activity of this catalyst, first, the reduction of 4-NP was checked in the presence of $NaBH_4$ and in absence of catalyst. No reduction reaction occurring in 2 h. In contrast, when the small amount of GO/Fe_3O_4/Pd nanocomposite was introduced into the reaction solution, the absorption peak at around 400 nm significantly decreased along with increasing a new absorption peak at ~ 300 nm immediately, as shown in Fig. 8a. Since, in this reaction, the amount of $NaBH_4$ is very high compare to 4-NP, ($C_{NaBH_4}/C_{4-NP} = 40$), the reaction rate can be

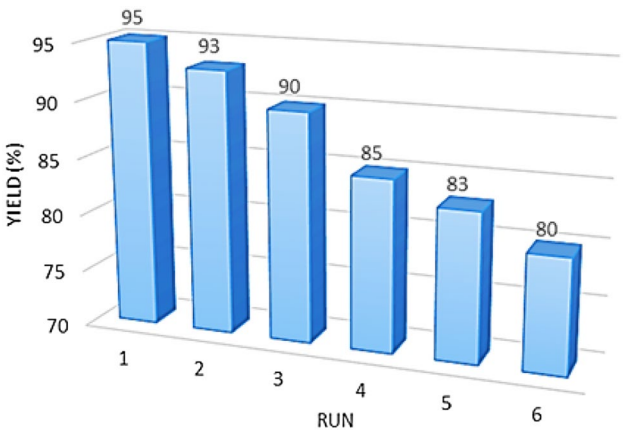

Fig. 7 Recyclability of (GO/Fe_3O_4/Pd nanocomposite) for the Suzuki–Miyaura coupling reaction of phenylboronic acid (1.1 mmol), iodobenzene (1 mmol), K_2CO_3 (2 mmol) and GO/Fe_3O_4/Pd nanocomposite (15 mg), EtOH/H_2O (4 mL), 80 °C, isolated yield after recrystallization

expected to be independent of the concentrations of borohydride and the reduction can be considered as a pseudo first order reaction with respect to the concentration of 4-NP

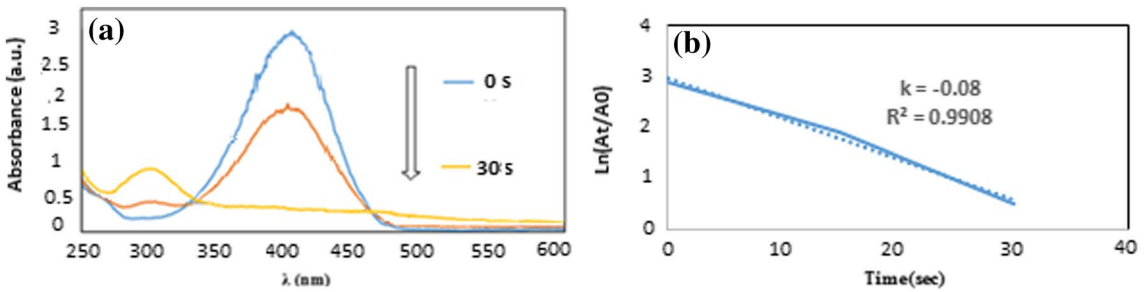

Fig. 8 Time dependent UV–Vis absorption spectra of 4-NP for the reduction of 4-NP. **a** In presence of (GO/Fe_3O_4/Pd nanocomposite) and $NaBH_4$. **b** Rate constant versus time in the presence of (GO/Fe_3O_4/Pd nanocomposite) and $NaBH_4$

Table 4 Comparison of literature results obtained with PdNP catalysts for the reduction of 4-nitrophenol in water

Entry	Catalyst	K_{app} (s^{-1})	Time (min)	Refs.
1	CNT/PiHP/Pd	5×10^{-3}	60	[64]
2	Ag@Pd/Fe_3O_4	3.3×10^{-2}	2	[65]
3	Pd–PEDOT	6.6×10^{-2}	1	[66]
4	SPB	4.41×10^{-3}	20	[67]
5	PPy/TiO_2/Pd	1.22×10^{-2}	7	[68]
6	SBA/Pd	1.2×10^{-2}	1	[69]
7	Mesoporous @Pd/CeO_2	8×10^{-3}	10	[70]
8	GO/Fe_3O_4/Pd nanocomposite	8×10^{-2}	0.5	This work

[63]. As the absorbance of 4-NP is proportional to its concentration, thus ln(Ct/C_0) versus time can be obtained based on the absorbance as the function of time (A_t/A_0 α C_t/C_0). The kinetic reaction rate constant (K) was calculated from the linear correlation between Ln (A_t/A_0) and time as shown in Fig. 8b.

We summarized some of the results which were reported in the literature for the reduction of 4-NP in the presence Pd catalysts. As shown, This catalyst acted with high efficiency compare to other reported catalysts (Table 4).

In the case of methylene blue and methyl orange changes in the color of the dye solution can be conveniently monitored by UV–Vis absorption spectroscopy. These investigations showed that partial reduction of MO and MB occurred for a long time (2 h) in presence of $NaBH_4$ alone. In contrast, upon addition of GO/Fe_3O_4/Pd nanocomposite (in the presence of $NaBH_4$), complete reduction was achieved within 10 and 20 s of reaction for MO and MB as can be seen in Figs. 9a, 10a respectively.

The kinetic data obtained for reduction of MO, MB were fitted to first-order rate equations. Herein the catalytic efficiency of (GO/Fe_3O_4/Pd nanocomposite) toward the degradation of the MO and MB studied and the calculated rate constants for reduction of these compounds were −0.087 and −0.575, which shown in Figs. 9b, 10b respectively.

Finally, in order to show the merit of this catalytic method, we compared our obtained results with other reported methods (Table 5), and found that the GO/Fe_3O_4/Pd nanocomposite is an equally or more efficient catalyst with respect to the reaction time and conversion than previously reported ones.

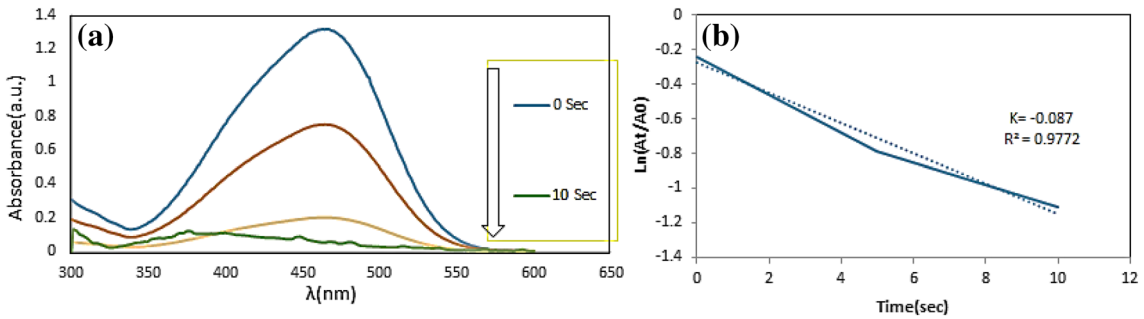

Fig. 9 Time dependent UV–Vis absorption spectra for the reduction of MB. **a** In presence of (GO/Fe_3O_4/Pd nanocomposite) and $NaBH_4$. **b** Rate constant versus time in presence of (GO/Fe_3O_4/Pd nanocomposite)

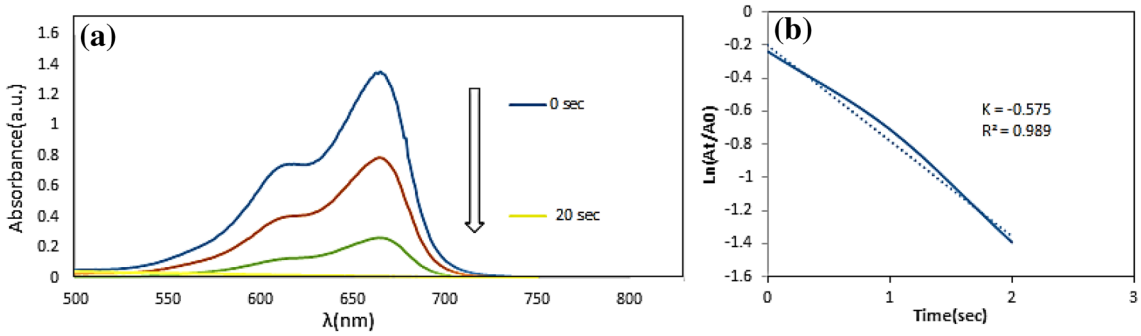

Fig. 10 **a** Time dependent UV–Vis absorption spectra of MB for the reduction of MB In the presence of (GO/Fe_3O_4/Pd nanocomposite) and $NaBH_4$. **b** Rate constant versus time in the presence of (GO/Fe_3O_4/Pd nanocomposite) and $NaBH_4$

Table 5 A comparison of the results of the present system with the literature precedents of some recently published catalytic systems for the reduction of variety of dyes by $NaBH_4$

Substrate	Catalyst	Time	Refs.
MO	Ag NPs/seashell	11 min	[71]
	GO/Pd nanocomposite	5 min	[72]
	Natrolite zeolite/Pd nanocomposite	5 min	[73]
	GO/Fe_3O_4/Pd nanocomposite	10 s	This work
MB	Au/Fe_3O_4@C	10 min	[74]
	Au core-PANI she	5 min	[75]
	Pd–PEI–RGO	5 min	[76]
	GO/Fe_3O_4/Pd nanocomposite	20 s	This work

3.4.2 Recyclability of (GO/Fe_3O_4/Pd Nanocomposite) in Reduction of 4-NP, MO and MB

The recyclability of catalyst (GO/Fe_3O_4/Pd nanocomposite) in reducing reaction of 4-NP, MO and MB in presence of $NaBH_4$ were investigated. The used catalyst can be recovered from the reaction mixture by using an external magnet, then washed and dried for the next cycle of catalysis. For reduction of these compounds, the catalyst exhibited similar catalytic performance without significantly reduction activity even after running ten cycles, as shown in Fig. 11. The amount of Pd loading in the 1 mg of used catalyst is 36×10^{-8} mol that was calculated by the ICP–AES analysis.

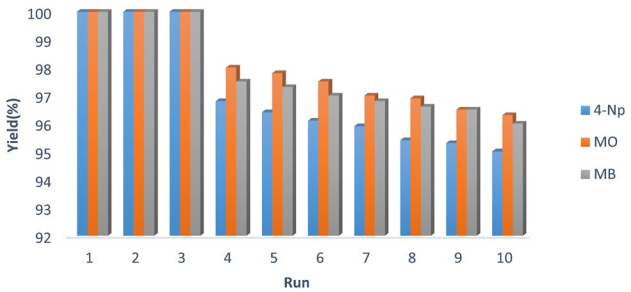

Fig. 11 Recycling of (GO/Fe_3O_4/Pd nanocomposite) for reduction of 4-NP, MB, MO under similar conditions

4 Conclusions

In summary, a simple, convenient and green process for the synthesis of GO/Fe_3O_4/Pd nanocomposite has been presented. Fabrication of this catalyst essentially includes several steps, firstly, the surface of synthesized GO was modified with several organic reagents such as: $SOCl_2$, 1,4-phenylenediamine, 2-pyridine carboxaldehyde. In the next steps, Pd^{2+} ion was coordinated with functionalized GO and reduced by leaf extract of *O. vulgare* to form Pd NPs. Finally this catalyst was magnetized by Fe_3O_4 NPs. The synthesized nanocatalyst is characterized by simple methods and demonstrates excellent catalytic activity for the carbon–carbon Suzuki–Miyaura cross-coupling reaction in an environmentally friendly solvent system. This catalyst present some advantages such as thermal stability of the catalyst, easy separation with external magnetic field, reusability of the catalyst for six times with minimal loss of activity, This catalyst also shown a broad range of utility for reduction of 4-NP, MO, MB by using $NaBH_4$ as a reducing agent at room temperature in aqueous media and retains its high activity for the degradation even after ten cycles.

Acknowledgements Thanks are due to the Iranian Nanotechnology Initiative and the Research Council of Shahid Bahonar University of Kerman and Chemistry Department for supporting of this work.

References

1. Alimardanov A, Schmieder-van de Vondervoort L, de Vries AH, de Vries JG (2004) Adv Synth Catal 346:1812–1817
2. Tsuji J (2006) Palladium reagents and catalysts: new perspectives for the 21st century. Wiley

3. Lamblin M, Nassar-Hardy L, Hierso JC, Fouquet E, Felpin FX (2010) Adv Synth Catal 352:33–79
4. Favier I, Madec D, Teuma E, Gomez MP (2011) Curr Org Chem 15:3127–3174
5. Wan Y, Wang H, Zhao Q, Klingstedt M, Terasaki O, Zhao D (2009) J Am Chem Soc 131:4541–4550
6. Tanaka S, Kaneko T, Asao N, Yamamoto Y, Chen M, Zhang W, Inoue A (2011) Chem Commun 47:5985–5987
7. Li Z, Lin S, Ji L, Zhang Z, Zhang X, Ding Y (2014) Catal Sci Technol 4:1734–1737
8. Parlett CM, Keshwalla P, Wainwright SG, Bruce DW, Hondow NS, Wilson K, Lee AF (2013) ACS Catal 3:2122–2129
9. Miyaura N, Yamada K, Suzuki A (1979) Tetrahedron Lett 20:3437–3440
10. Campeau L-C, Fagnou K (2006) Chem Commun 1253–1264
11. Baudoin O, Cesario M, Guenard D, Guéritte F (2002) J Org Chem 67:1199–1207
12. Torborg C, Beller M (2009) Adv Synth Catal 351:3027–3043
13. Suzuki M, Yamato Y, Akiyama T (1977) Water Res 11:275–279
14. Lee D-H, Jin M-J (2010) Org Lett 13:252–255
15. Mandali PK, Chand DK (2013) Catal Commun 31:16–20
16. Heugebaert TS, De Corte S, Sabbe T, Hennebel T, Verstraete W, Boon N, Stevens CV (2012) Tetrahedron Lett 53:1410–1412
17. Peng Y-Y, Liu J, Lei X, Yin Z (2010) Green Chem 12:1072–1075
18. Wei S, Dong Z, Ma Z, Sun J, Ma J (2013) Catal Commun 30:40–44
19. Sakurai H, Tsukuda T, Hirao T (2002) J Org Chem 67:2721–2722
20. Bhanage BM, Arai M (2001) Catal Rev 43:315–344
21. Köhler K, Heidenreich RG, Soomro SS, Pröckl SS (2008) Adv Synth Catal 350:2930–2936
22. Srivastava R, Venkatathri N, Srinivas D, Ratnasamy P (2003) Tetrahedron Lett 44:3649–3651
23. Djakovitch L, Koehler K (2001) J Am Chem Soc 123:5990–5999
24. Djakovitch L, Koehler K (1999) J Mol Catal A 142:275–284
25. Narayanan R, El-Sayed MA (2003) J Am Chem Soc 125:8340–8347
26. Narayanan R, El-Sayed MA (2004) J Phys Chem B 108:8572–8580
27. Scheuermann GM, Rumi L, Steurer P, Bannwarth W, Mülhaupt R (2009) J Am Chem Soc 131:8262–8270
28. Rumi L, Scheuermann GM, Mülhaupt R, Bannwarth W (2011) Helv Chim Acta 94:966–976
29. Siamaki AR, Abd El Rahman SK, Abdelsayed V, El-Shall MS, Gupton BF (2011) J Catal 279:1–11
30. Makharza S, Cirillo G, Bachmatiuk A, Ibrahim I, Ioannides N, Trzebicka B, Hampel S, Rümmeli MH (2013) J Nanopart Res 15:2099
31. Ramasamy MS, Mahapatra SS, Cho JW (2015) J Colloid Interface Sci 455:63–70
32. Jing Q, Liu W, Pan Y, Silberschmidt VV, Li L, Dong ZC (2015) Mater Des 85:808–814
33. Pan Y, Bao H,. Sahoo NG, Wu T, Li L (2011) Adv Funct Mater 21:2754–2763
34. Lee SH, Dreyer DR, An J, Velamakanni A, Piner RD, Park S, Zhu Y, Kim SO, Bielawski CW, Ruoff RS (2010) Macromol Rapid Commun 31:281–288
35. Jia L, Zhang Q, Li Q, Song H (2009) Nanotechnology 20:385601
36. Petla RK, Vivekanandhan S, Misra M, Mohanty AK, Satyanarayana N (2012) J Biomater Nanobiotechnol 3:14–19
37. Sathishkumar M, Sneha K, Kwak IS, Mao J, Tripathy S, Yun Y-S (2009) J Hazard Mater171:400–404
38. Yang X, Li Q, Wang H, Huang J, Lin L, Wang W, Sun D, Su Y, Opiyo J. Hong B L (2010) J Nanopart Res 12:1589–1598
39. Sathishkumar M, Sneha K, Yun YP (2009) Int J Mater Sci 4:11–17
40. Veisi H, Faraji AR, Hemmati S, Gil A (2015) Appl Organomet Chem 29:517–523
41. Khazaei A, Rahmati S, Hekmatian Z, Saeednia S (2013) J Mol Catal A 372:160–166
42. Veisi H, gorbani-Vaghei R, Hemmati S, Aliani M. Ozturk H T (2015) Appl Organomet Chem 29:26–32
43. Petcharoen K, Sirivat A (2012) Mater Sci Eng B 177:421–427
44. Marcano DC, Kosynkin DV, Berlin JM, Sinitskii A, Sun Z, Slesarev A, Alemany LB, Lu W, Tour JM (2010) ACS Nano 4:4806–4814
45. Hummers WS Jr, Offeman RE (1958) J Am Chem Soc 80:1339–1339
46. Humers W, Offeman R (1958) J Am Chem Soc 80:1339
47. Zu S-Z, Han B-H (2009) J Phys Chem C 113:13651–13657
48. Titelman GI, Gelman V, Bron S, Khalfin RL, Cohen Y, Bianco-Peled H (2005) Carbon 43:641–649
49. Gromov A, Dittmer S, Svensson J, Nerushev OA, Perez-García SA, Licea-Jiménez L, Rychwalski R, Campbell EE (2005) J Mater Chem 15:3334–3339
50. Yang Y, Wan M (2002) J Mater Chem 12:897–901
51. Fang M, Wang K, Lu H, Yang Y, Nutt S (2009) J Mater Chem 112:7098–7105
52. Kemikli N, Kavas H, Kazan S, Baykal A, Ozturk R (2010) J Alloy Compd 502:439–444
53. Petla RK, Vivekanandhan S, Misra M, Mohanty A. K, Satyanarayana N (2011) J Biomater Nanobiotechnol 3:14–19
54. Das DD, Sayari A (2007) J Catal 246:60–65
55. Shiyong L, Qizhong Z, Zhengneng J, Huajiang J, Xuanzhen J (2010) Chin J Catal 31:557–561
56. Yang X, Fei Z, Zhao D, Ang WH, Li Y, Dyson P (2008) J Inorg Chem 47:3292–3297
57. Kim SW, Kim M, Lee WY, Hyeon T (2002) J Am Chem Soc 124:7642–7643
58. Hekmati M, Bonyasi F, Javaheri H, Hemmati S (2017) Appl Organomet Chem e3757:1–7
59. Kwon TH, Cho K, Baek Y, Yoon KY, Kim HG B. M (2017) RSC Adv 7:11684–11690
60. Nie R, Shi J, Du W, Hou Z (2014) Ni_2O_3-around-Pd hybrid on graphene oxide. Appl Catal A 473:1–6
61. Jafar Hoseini S, Ghanavat Khozestan H, Hashemi Fath R (2015) RSC Adv 5:47701–47708
62. Karical RG, James KW, Fox M (2013) Nano Lett 3:1757–1760
63. Gazi S, Ananthakrishnan R (2011) Appl Catal B 105:317–325
64. Li H, Han L, Cooper-White J, Kim I (2012) Green Chem 14:586–591
65. Jiang K, Zhang HX, Yang YY, Mothes R, Lang H, Cai WB (2011) Chem Commun 47:11924–11926
66. Harish S, Mathiyarasu J, Phani KLN, Yegnaraman V (2009) J Catal Lett 128:197–202
67. Mei Y, Lu Y, Polzer F, Ballauff M, Drechsler M (2007) Chem Mater 19:1062–1069
68. Lu X, Bian X, Nie G, Zhang C, Wang C, Wei Y (2012) J Chem Mater 22:12723–12730
69. Morere J, Tenorio MJ, Torralvo MJ, Pando C, Renuncio JAR, Cabanas A (2011) J Supercrit Fluids 56:213–222
70. Bhandari R, Knecht MR (2011) ACS Catal 1:89–98
71. Ghosh BK, Hazra S, Naik B, Ghosh NN (2015) Powder Technol 269:371–378
72. Omidvar A, Jaleh B, Nasrollahzadeh M (2017) J Colloid Interface SCI 496:44–50
73. Hatamifard A, Nasrollahzadeh M, Lipkowski J (2015) RSC Adv 5:91372–91381
74. Dutt S, Siril P. Sharma F, Periasamy V S (2015) New J Chem 39:902–908
75. Feng H, Zheng-yi Z, Yao X, Wu-xiang W, Ya-fang H, Run W (2000) Acta Metall Sin 36:659–661
76. Li S, Li H, Liu J, Zhang H, Yang Y, Yang Z, Wang L, Wang B (2015) Dalton Trans 44:9193–9199